

X-ray Power Density Spectrum of the Narrow Line Seyfert 1 Galaxy Akn 564

Ken Pounds¹, Rick Edelson^{1,2}, Alex Markowitz², Simon Vaughan^{1,3}

kap@star.le.ac.uk

ABSTRACT

Beginning in 1999 January, the bright, strongly variable Narrow-Line Seyfert 1 (NLS1) galaxy Akn 564 has been observed by *RXTE* once every ~ 4.3 days. It was also monitored every ~ 3.2 hr throughout 2000 July. These evenly-sampled observations have allowed the first quantitative comparison of long and short time-scale X-ray variability in an NLS1 and the derivation of an X-ray Power Density Spectrum (PDS). The variability amplitude in the short time-scale light curve is very similar to that in the long time-scale light curve, in marked contrast to the stronger variability on longer time-scales which is characteristic of “normal” broad-line Seyfert 1s (BLS1s). Furthermore, the Akn 564 PDS power law cuts off at a frequency of 8.7×10^{-7} Hz corresponding to a timescale of ~ 13 d, significantly *shorter* than that seen in the PDS of NGC 3516, a BLS1 of comparable luminosity.

This result is consistent with NLS1s showing faster (as opposed to larger amplitude) variations than BLS1s, providing further evidence that NLS1s harbour lower mass black holes than BLS1s of similar luminosity, accreting at a correspondingly higher relative rate.

Subject headings: galaxies: active — galaxies: individual (Akn 564) — galaxies: Seyfert — X-rays: galaxies

1. Introduction

A relatively recent development in the taxonomy of active galactic nuclei (AGN) has been the emergence of Narrow-Line Seyfert 1 (NLS1) galaxies as an important sub-class. NLS1s were originally identified on the basis of their optical properties: exhibiting narrower permitted lines ($H\beta$ FWHM < 2000 km/s) than “normal” Broad-Line Seyfert 1s (BLS1s) and weaker $[O\ III]/H\beta < 3$ than Seyfert 2s (Osterbrock & Pogge 1985; Goodrich 1989). *ROSAT* data showed these properties to be strongly correlated with X-ray spectral slope, in the sense that NLS1s tend to have steep soft

¹X-ray Astronomy Group; University of Leicester; Leicester LE1 7RH; United Kingdom

²Astronomy Department; University of California; Los Angeles, CA 90095-1562; USA

³Institute of Astronomy; University of Cambridge; Cambridge CB3 0HA; United Kingdom

X-ray spectra (Boller et al. 1996). In addition, many NLS1s are strongly variable on time-scales of hours or less, with some NLS1s showing giant (factor of ~ 100) X-ray flares over time-scales of days (e.g., Brandt et al. 1999). On these short time-scales the variability levels in NLS1s are typically a factor of ~ 3 – 10 times larger than those seen in BLS1s of similar luminosity (Turner et al. 1999; Leighly 1999).

A number of models have been proposed to explain the distinctive properties observed in NLS1s. The most widely accepted explanation is that NLS1s are accreting near the Eddington limit (Pounds et al. 1995, Laor et al. 1997), while BLS1s accrete at a lower rate. On this interpretation the high accretion rate is directly responsible for the strong soft X-ray emission, by enhanced thermal radiation from the accretion disc, while the increased soft photon flux cools the hard X-ray source leading to the steeper power law frequently seen at higher X-ray energies in NLS1s (Brandt et al. 1997). It is the prospect that comparative study of NLS1s and BLS1s will shed light on the accretion rate, one of the fundamental parameters of an AGN, that makes the emergence of the new sub-class of AGN of such interest and importance.

X-ray variability has been recognised as a powerful probe of the central regions of AGN since the *EXOSAT* “long-looks” first showed (McHardy 1988) that rapid variability was common in Seyfert galaxies, lending early support to the now-standard black hole/accretion disc paradigm. The *EXOSAT* data were found to be well-described by a fluctuation power density spectrum (PDS) rising smoothly to lower frequencies as a power law, $f^{-\alpha}$ where $\alpha = 1 - 2$, to a limit imposed by the maximum duration of the ~ 2 -day observations (e.g., Lawrence & Papadakis 1993). Attempts to constrain a flattening or “cut-off” in the PDS (as required to avoid the variability power diverging) were made by combining *EXOSAT* data with earlier X-ray satellite observations of NGC 5506 (McHardy 1988) and NGC 4151 (Papadakis and McHardy 1995). These analyses yielded evidence for a cut-off time-scale of several weeks; however, the uneven sampling of these data made their reliability uncertain. The observational situation was significantly improved with the launch of *RXTE*. Taking advantage of the unique properties of this satellite, Edelson and Nandra (1999) obtained evenly-sampled fluxes of the BLS1 NGC 3516 on long, medium and short time-scales, and combined these data to produce a PDS covering 4 decades in temporal frequency, finding a cut-off time-scale of ~ 1 month.

Until now the only quantitative assessment of the rapid X-ray variability of NLS1s has been based on measurements of the excess variance, obtained from *ASCA* observations, typically of 1 day duration. Based on these data, Turner et al. (1999) and Leighly (1999) found the short-term variability of NLS1s to be substantially greater than for BLS1s, while in both cases the excess variance was anticorrelated with the X-ray luminosity. The present paper reports the results of the first extensive and evenly-sampled X-ray monitoring of an NLS1, using *RXTE* to monitor Akn 564 over a near 2-year period. Akn 564 is particularly well suited for this study, being the brightest known NLS1 in the hard X-ray sky ($F(2 - 10 \text{ keV}) \approx 2 - 5 \times 10^{-11} \text{ erg cm}^{-2} \text{ sec}^{-1}$; Vaughan et al. 1999a), strongly variable (e.g., 50% variations on timescales of hours; Leighly 1999) and located well out of the ecliptic plane (allowing monitoring by *RXTE* throughout the year). Subsequent

to the start of our *RXTE* monitoring campaign, Akn 564 was chosen for simultaneous monitoring with *HST*, *ASCA*, *Chandra* and the AGN Watch network of ground based optical telescopes.

2. Observations and Data Reduction

Our X-ray monitoring was planned to obtain variability information spanning time-scales from hours to months. Akn 564 was observed once every 4.3 days (= 64 orbits) from 1999 January 1 – 2000 September 19 (the limit of the present analysis, although this low-frequency monitoring is continuing), and once every ~ 3.2 hr (= 2 orbits) from 2000 June 30 – August 1. (Twice-daily observations were also obtained during 1999 October 25 – November 11, in support of the AGN Watch campaign; Schemmer et al. in preparation). Our sampling parameters are summarized in Table 1.

The *RXTE* Proportional Counter Array (PCA) consists of five collimated Proportional Counter Units (PCUs), sensitive in a nominal 2–60 keV bandpass (Jahoda et al. 1996). At the start of the present campaign three of the PCUs (0, 1 and 2) were in routine use. After the gain settings of all five PCUs on board *RXTE* were changed on 1999 March 22 this number was reduced to two (0 and 1), and then, from 2000 May 12, to one (1). Data collected during each of the two gain epochs were extracted separately using background model files appropriate to that gain epoch. The present analysis is restricted to the 2–10 keV band, where the PCA is most sensitive and the systematic errors are best understood. Data from the top (most sensitive) layer of the PCU array were extracted using the REX reduction script⁴, and background counts were estimated using the “L7–240” model⁵. Background-subtracted count rates were then obtained in each epoch to assign a mean flux and error. Count rates derived from data taken during the earlier gain setting were scaled to account for the effect of the gain change by a factor derived from observations of Cassiopeia A, and then normalised to units of $\text{ct s}^{-1} \text{PCU}^{-1}$. Figure 1 (top panel) reproduces the full light curve.

3. Temporal Analysis

Before performing the time series analyses described below, the observed light curve was re-sampled to provide two nearly-independent light curves, one sampling short time-scales (\sim days) and the other, long time-scales (\sim months). In Figure 1, the centre panel contains the full 20 months of data, sampled on a grid as close to 4.3 d as possible. Interpolating over the 9 data points that were missing during this period and mapping to an even grid yielded a total of 148 evenly-spaced flux points. This had the effect of filtering out (not smoothing) most of the data in the intensive periods around MJD 51480 and 51700. The short time-scale light curve, shown in the bottom

⁴See <http://heasarc.gsfc.nasa.gov/docs/xte/recipes/rex.html>

⁵See <http://lheawww.gsfc.nasa.gov/~keith/dasmith/rossi2000/index.html>

panel of Figure 1, was obtained during the 32 d intensive sampling period 2000 June 30 – August 1. Interpolating over the 13 data points missing during this period yielded a total of 235 evenly-spaced flux points.

3.1. Comparison of Long and Short Timescale Light Curves

The long and short time-scale data are quantitatively compared in Table 2, where column 2 gives the mean count rates, and column 4 the fractional excess variance, σ_{XS}^2 , defined as

$$\sigma_{XS}^2 = \frac{S^2 - \langle \sigma_{err}^2 \rangle}{\langle X \rangle^2}, \quad (1)$$

where $\langle X \rangle$ is the mean flux, $\langle \sigma_{err}^2 \rangle$ is the mean square error, and S^2 is the measured variance of the light curve (e.g. Nandra et al. 1997). We have estimated ($\pm 1\sigma$) errors on the excess variance as $\pm \sigma_{XS}^2 \sqrt{2/N}$, where N is the number of flux points, noting that for Gaussian fluctuations S^2 will follow a χ^2 distribution (Warwick, private communication).

The short time-scale light curve of Akn 564 shows a marginally *larger* excess variance than the long time-scale light curve, a result that is strikingly different from that of BLS1s. In a survey of *RXTE* and *ASCA* data for 8 BLS1s, Markowitz & Edelson (2001) found larger values of σ_{XS}^2 on long (\sim months) than on short (\sim hours) time-scales in every case. This comparison strongly suggests that large amplitude X-ray variability is more rapid, i.e., extends to significantly shorter time-scales, in Akn 564 than in BLS1s of comparable luminosity.

3.2. Fluctuation Power Density Spectrum

In order to better quantify the short-term variability of Akn 564 the PDS was then constructed following the prescription of Edelson & Nandra (1999), first determining separate short and long time-scale PDS and then combining them to produce a single PDS. The individual PDS were derived using a direct Discrete Fourier Transform (Oppenheim & Shafer 1975, Brillinger 1981). The zero-power and next two (very noisy) lowest-frequency points of each PDS were ignored and the remaining points binned every factor of 1.7 (0.23 in the logarithm). Power-law models were then fitted separately to the long and short time-scale PDS. The slope and uncertainty, measured from an unweighted, least-squares fit to the logarithmically binned data, and derived using the Welch window function, are given in column 5 of Table 2. These show a highly significant (10σ) systematic flattening from short time-scales (with $a = -0.96 \pm 0.07$) to long time-scales ($a = -0.24 \pm 0.08$).

The long and short time-scale PDS were then combined. Unlike Edelson & Nandra (1999), who allowed the relative normalization between PDS to float as a free parameter, the absolute normalizations were retained. The combined PDS is shown in Figure 2. A simple power law gave an unacceptable fit ($>99.99\%$), with a reduced chi-squared of $\chi^2_{\nu} = 3.06$ for 13 degrees of freedom.

The combined PDS was then fitted with a model in which a steep power law dominates at high frequencies, but cuts off to a slope of $a = 0$ at low frequencies:

$$P(f) = C/(1 + f/f_c)^a, \quad (2)$$

where $P(f)$ is the fluctuation power at a frequency f , a is the power law slope at high temporal frequencies, f_c is the “cutoff frequency,” well below which the PDS flattens to a slope of zero, and C is the normalization. The fit, with three free parameters (C , f_c , and a) was a significant improvement over the simple power law, with $\chi^2_\nu = 1.70$ for 12 degrees of freedom, although still formally unacceptable (94% confidence) mainly due to the higher absolute level of variability power in the short time-scale data. The high-frequency slope of the broken power law fit is $a = -1.12$, similar to the slope derived using the high-frequency PDS alone, and the cutoff frequency of 8.7×10^{-7} Hz corresponds to a timescale of ~ 13 d. These parameters are summarized in Table 3. While the power law plus cutoff model is clearly a marked improvement over the unbroken power law, we note the exact shape of the turnover is not well constrained and the low-frequency behaviour not at all well determined.

4. Discussion and Conclusions

We have carried out the most comprehensive X-ray variability study of an NLS1 to date. The long and short time-scale light curves of Akn 564 are found to be remarkably similar, with comparable excess variances over the sampling intervals of 32 days and 627 days. The straightforward deduction from a visual examination of the light curves is that Akn 564 exhibits most of its variability power on time-scales substantially less than one month. We suggest this may well be a common feature of NLS1s, and one which distinguishes the sub-class from BLS1s. Turner et al. (1999) calculated the excess variance for *ASCA* observations of 36 Seyfert galaxies over a typical sampling interval of 1 day finding values up to ~ 10 times greater for NLS1s compared with BLS1s (of similar luminosity). A current explanation for the rapid and large amplitude variability characteristic of Narrow Line AGN is in terms of a smaller black hole mass, and hence of size scale. Our result now confirms - for Akn 564 - that the large short-term variability is indeed primarily due to the time-scales being shorter (rather than - necessarily - having greater variability power) than for BLS1 of comparable luminosity.

The Akn 564 PDS now offers an opportunity to quantify the lower mass and higher accretion rate of a NLS1 in comparison with a BLS1 of similar luminosity. To date the only BLS1 PDS obtained by a similar evenly-sampled campaign is for NGC 3516, from which Edelson & Nandra (1999) obtained a cut-off time-scale of ~ 30 d. Assuming for the moment a simple scaling law applies for the variability time-scale and black hole mass of NLS1 and BLS1, our result suggests that Akn 564 has a black hole mass of order ~ 0.4 that of NGC 3516. Reverberation mapping by Robinson et al. (1994) found NGC 3516 to have a black hole mass of order $\sim 3 \times 10^7 M_\odot$, implying a corresponding mass for Akn 564 of $\sim 1 \times 10^7 M_\odot$. Estimation of the accretion rate for most

AGN is hampered by a large uncertainty of the luminosity in the hidden EUV band. However, Wandel et al. (1999) showed the bolometric luminosity of BLS1s may be estimated by scaling from the continuum luminosity at 5100 \AA , based on a comparison of photoionisation and reverberation estimates of black hole masses. By this means we derive a bolometric luminosity for NGC 3516 of $\sim 10^{44} \text{ erg/s}$ which should be good to a factor of ~ 3 . The corresponding accretion rate for NGC 3516 is then of order $0.05 \dot{M}_{\text{Edd}}$.

The very different SED of NLS1s means we cannot rely on the Wandel et al. (1999) relation to estimate the bolometric luminosity of Akn 564. Instead we use the respective 2–10keV luminosities, for which Akn 564 is some ~ 3 times that of NGC 3516. Combining the respective estimates of black hole mass and luminosity then gives an accretion rate some ~ 8 times larger for Akn 564 than for NGC 3516, indicating that Akn 564 is accreting at a substantial fraction of the Eddington limit, or $0.4 \dot{M}_{\text{Edd}}$. We note furthermore that this is probably a lower limit, given that the scaling with NGC 3516 via the 2–10 keV luminosities takes no account of the strong soft X-ray excess in Akn 564.

Interpreting the PDS in the above way is subject to two caveats. First, is the variability stationary, to at least the extent that the measured "characteristic time-scale" is a reliable measure of scale and black hole mass? The uniformity of the long time-scale light curve of Akn 564 shown in Figure 1 is reassuring in that respect, suggesting the absence of low frequency power is sustained throughout our campaign. On the other hand, the higher mean flux and larger fractional variability during the intensive monitoring suggests a degree of non-stationarity, but not to an extent which alters our basic finding, that Akn 564 contains most of its variability power on timescales much shorter than 1 month. A second question is whether the accretion discs in both Akn 564 and NGC 3516 extend close to the innermost stable orbit, justifying our inverse scaling of black hole mass with the respective values of f_c ? The high luminosity of NLS1s indicate that is generally true for NLS1s, while in the case of NGC 3516 the observation of a broad Fe-K fluorescence line (Nandra et al. 1999) suggests that its accretion disc also extends close to the innermost stable orbit.

We conclude that comparisons of the X-ray variability of Akn 564 and NGC 3516 indicate a black hole mass for Akn 564 of $\sim 1 \times 10^7 M_{\odot}$, implying an accretion rate in the range 0.2–1.0 \dot{M}_{Edd} . It is interesting to compare this result with the accretion rate derived from modelling of line widths and variability time-scales in the optical Broad Line Region (Laor 1998). Taking the above estimate for the luminosity of Akn 564 and $H\beta$ FWHM = 800 km/s (Vaughan et al. 1999b), the relation in Laor (1998) yields an "independent" estimate for Akn 564 of $1.0 \dot{M}_{\text{Edd}}$

The authors acknowledge the dedicated work of the *RXTE* team, especially Evan Smith for his careful scheduling so close to the ephemeris. RAE and AM were supported by NASA grants NAG 5-7315 and NAG 5-9023, and SAV by the UK Particle Physics and Astronomy Research Council.

REFERENCES

- Boller,Th.,Brandt,W.N. & Fink,H. 1996, A&A, 305, 53
- Brandt,W.N.,Mathur,S. & Elvis,M. 1997, MNRAS, 285, 25P
- Brandt, W.N.,Boller,Th.,Fabian,A.C. & Ruszkowski, M. 1999, MNRAS,303,L53
- Brillinger, D., 1981 “Time Series: Data Analysis and Theory,” 2nd Edition (Holden-Day Publishing)
- Edelson, R. & Nandra, K. 1999, ApJ, 514, 682
- Goodrich, R.W. 1989, ApJ, 342, 234
- Jahoda, K., Swank, J., Giles, A., Stark, M., Strohmayer, T., Zhang, W., Morgan, E.H. 1996, SPIE 2808, 59
- Laor, A. et al. 1997, ApJ, 477, 93
- Laor, A. 1998, ApJ, 505, L83
- Leighly, K. 1999, ApJS, 125, 297
- Lawrence, A. & Papadakis, I. 1993, ApJ, 414, L85
- Markowitz, A. & Edelson, R. 2001, ApJ, in press
- McHardy, I. 1988, Mem Soc Ast Ital, 59, 239
- Nandra, K.,George,I.M.,Mushotzky, R.F.,Turner,T.J. & Yaqoob, T. 1997, ApJ, 476, 70
- Nandra, K.,George,I.M.,Mushotzky, R.F.,Turner,T.J. & Yaqoob, T. 1999, ApJ, 523, L17
- Oppenheim, A. & Shafer, R. 1975, “Digital Signal Processing,” (Prentice-Hall Publishing)
- Osterbrock, D.E. & Pogge, R.W. 1985, ApJ, 297, 166
- Papadakis, I. & McHardy, I. 1995, MNRAS, 273, 923
- Pounds,K.A., Done,C. & Osborne, J. 1995, MNRAS, 277, L5
- Robinson, A. 1994, ASP Conf Ser, 69, 147
- Turner, T.J.,George,I.M.,Nandra,K. & Turcan,D. 1999, ApJ, 524, 667
- Vaughan, S.,Pounds,K.A.,Reeves,J.N.,Warwick,R.S. & Edelson,R.A. 1999a, MNRAS, 308, L34
- Vaughan, S.,Reeves,J.N.,Warwick,R.S. & Edelson,R.A. 1999b, MNRAS, 309, 113
- Wandel, A.,Peterson,B.M. & Malkan,M.A. 1999, MNRAS, ApJ, 526, 579

Table 1. Sampling Parameters

Time Scale	Observing Dates (MJD)	Mean Sampling Interval	Data Lost	No. of Flux Points	Usable Temporal Frequency Range
Long	51179.55–51806.78	4.267 d	9 points	148	$6.9 \times 10^{-8} - 1.1 \times 10^{-6}$
Short	51694.82–51726.47	3.2 hr	13 points	235	$1.4 \times 10^{-6} - 3.4 \times 10^{-5}$

Table 2. Multi-Band Light Curve Properties

Time Scale	Mean ct s^{-1}	Excess Variance	Power-Law Slope
Long	1.63 ± 0.04	0.076 ± 0.009	-0.24 ± 0.08
Short	1.87 ± 0.04	0.111 ± 0.010	-0.96 ± 0.07

Table 3. PDS Fit Parameters

Description	Parameter	value
High-Frequency Slope	a	-1.12 ± 0.04
Cutoff Frequency	f_c	$8.72 \pm 0.81 \times 10^{-7} \text{ Hz}$
Cutoff Timescale	$t_c (= 1/f_c)$	$13.3_{-1.2}^{+1.3} \text{ days}$
Normalization Coefficient	C_1	$4.4 \pm 0.2 \times 10^6 \text{ Hz}^{-1}$

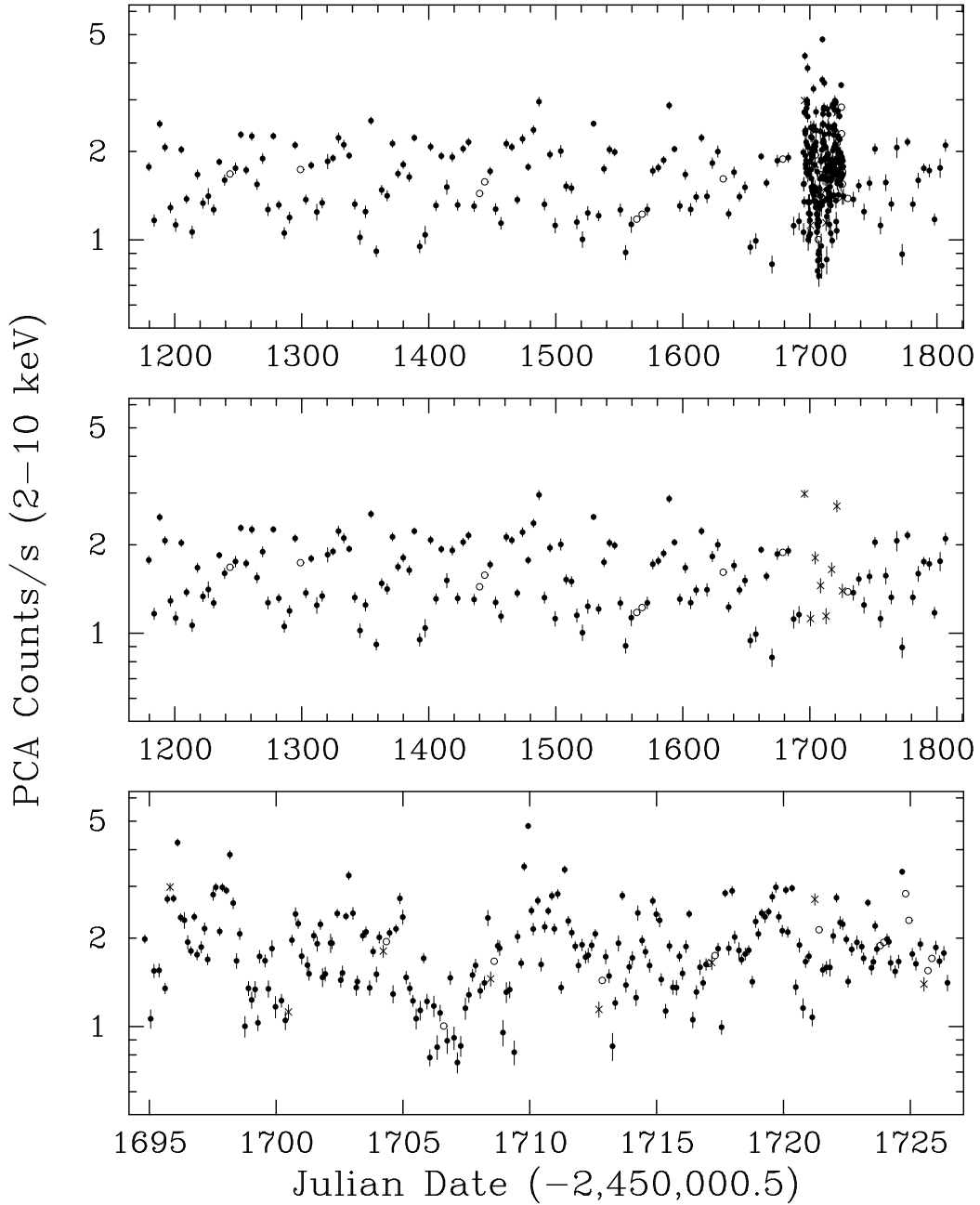


Fig. 1.— Full band (2-10 keV) light curve (top), resampled on long (4.3 d-20 months; centre) and short (3.2 hr-31 d; bottom) timescales. These middle and lower light curves were produced by filtering and interpolating the data in the top panel as described in the text. Interpolated points are shown as open circles without error bars, and the 8 points common to both light curves as \times 's.

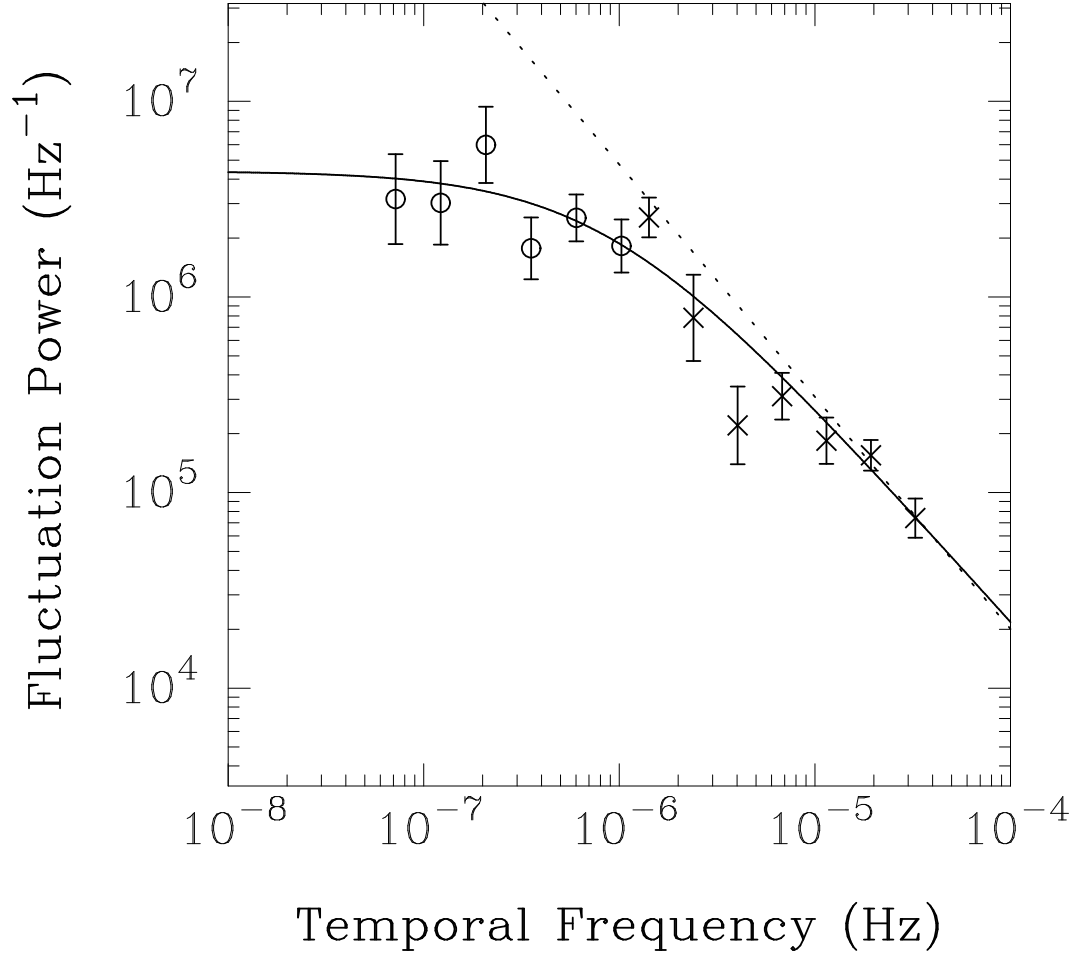


Fig. 2.— The combined PDS of Akn 564. The crosses refer to the PDS derived from the short term light curve while the circles are from the long timescale PDS. The solid line is the best fit as described in the text, a power-law with a low-frequency cutoff at ~ 13 d. The dotted line is the same power-law without the cutoff.